Stop A3/2

THE CRETACEOUS-PALEOGENE (K/PG) BOUNDARY AT THE GAMSBACH SECTION (GAMS, STYRIA)

Hans Egger, Christian Koeberl, Omar Mohamed, Christoph Spöttl, Michael Wagreich

Topics:

Cretaceous/Paleogene-boundary, nannoplankton, dinoflagellates, geochemistry

Tectonic unit:

Northern Calcareous Alps

Lithostratigraphic unit:

Nierental Formation

Chronostratigraphic units:

Upper Maastrichtian to lowermost Paleocene

Biostratigraphic units:

Calcareous nannoplankton Zones CC26 and NP1

Location:

Gamsbach to the east of Haid (Gams, Styria)

Coordinates:

E 014° 51′ 50″ N 47° 39′ 51″)

References:

Egger et al., 2009c

Introduction

In the area east of Gams (Styria, Austria), the Cretaceous/Paleogene boundary has been recognized in the Gamsbach section, which comprises the upper part of the Cretaceous *Nephrolithus frequens* Zone (CC26) and the lower part of the Paleocene *Markalius inversus* Zone (NP1). The 6.5 m long section is part of the Nierental Formation of the Gosau Group of the Northern Calcareous Alps.

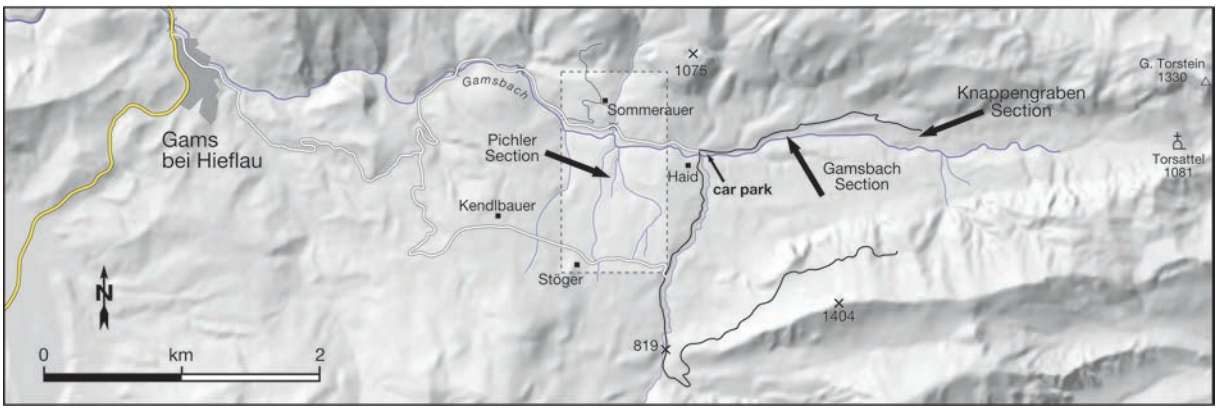

Figure A3.4 ▲
Positions of the Gamsbach (Stop A3/2), Pichler (StopA3/3) and Knappengraben sections.

The Gosau Group of Gams comprises deposits of Late Turonian to Eocene age (e.g., Wicher 1956; Kollmann 1964; Egger and Wagreich 2001; Egger et al. 2004), and rests on top of the Tyrolian nappe system. Up to 1000 m of terrestrial to shallow-marine strata of the Lower Gosau Subgroup (Upper Turonian - Santonian) occur in the western outcrop area near the village Gams. Deep-water sediments of the Nierental Formation (Upper Gosau Subgroup; mainly turbidites and hemipelagites) rest unconformably upon a relatively thin Santonian/Campanian succession in the eastern outcrop area of the Cretaceous.

Foraminifera of the Knappengraben section (1.25 km to the east of the Gamsbach section -Fig. A3.4; Tab. 1) were described by Rögl (in Egger et al. 2004) and indicate deposition in a middle bathyal environment (600 m to 1000 m paleodepth) during the latest Maastrichtian to earliest Danian (Biozones P0 – Pα following the zonation of Olsson et al. 1999). The lower Danian deposits (Biozone P1a) were probably accumulated at lower bathyal paleodepths (1000 m to 2000 m). The top of Zone P1a corre-

Section GG-75 sample no./ position above Cretaceous/Paleogene boundary	Rö 18/88 top Cretaceous	Rö 101/86/1A 0.0-0.5 cm	Rö 101/86/1B 0.5-0.7 cm	Rö 19-88 4 cm	Rö 103/86 10-15 cm	Rö 20/88 15-22 cm	Rö 21/88 25-30 cm	Rö 22/88 50-55 cm	Rö 23/88 65-70 cm	Preisinger 77.0-78.5 cm	Rö 24/88 80-85 cm	Rö 25/88 86-95 cm	Rö 26/88 95-100 cm	Rö 27/88 100-110 cm	Rö 28/88 127-133 cm	Rö 30/88 151-160 cm	Rö 31/88 181-186 cm	Rö 32/88 200-205 cm	Rö 33/88 250-255 cm	Rö 35/88 350-550cm	Rö 36/88 550-555 cm	Rö 38/88 675-680 cm	Rö 40/88 800-805 cm
Parvularugoglobigerina eugubina	Maastrichtian *A. mayaroensis* Zone	Reworking of Upper Cretaceous	Reworking of Upper Cretaceous	cf	x	x	x	x	Agglutinated assemblage	x	x	x	x	x	Agglutinated assemblage		x	x	x	Marl pebble layer and slump	x	x	x
Globoconusa daubjergensis				cf		cf				x	cf		x	x		x	x	x	x		x	x	x
Parvularugoglobigerina sabina				Bathyal benthic assemblage	x	x	x			x		x	x	x		x	x	x	x		x	x	x
Eoglobigerina edita					x			x		x	x	x	x	x			x	x	x		x	x	
Parasubbotina cf. *pseudobulloides*					x			x		x		x				x	x	x	x			x	x
Subbotina triloculinoides					cf								x	x		x		x				x	x
Guembelitria cretacea					x	x	x	x		x	x		x	x		x	x	x	x		x	x	
Woodringina claytonensis					x			x		x	x	x	x	x		x	x	x	x		x	x	x
Woodringina hornerstownensis					x			x		x		x	x	x		x	x	x	x		x	x	x
Chiloguembelina midwayensis					x		x			x		x	x	x		x		x	x			x	x
Chiloguembelina morsei						x				x	x		x	x		x	x	x	x			x	x
Parasubbotina pseudobulloides										x		x		x								x	
Eoglobigerina eobulloides											x	x	x	x		x		x	x		cf	x	
Subbotina trivialis													x	x		x	x		x			x	x
Praemurica pseudoinconstans														x		x						x	
Praemurica taurica														x								x	
Biostratigraphic Zonation		P0			Pα								P1a										

Table 1 ▲
Distribution of Foraminifera at the Knappengraben section

Figure A3.5 ►
Planktonic foraminifera from the Knappengraben section:

1 *Globoconusa daubjergensis* (Brönnimann)
GG-75, 882-897 cm
2 *Parvularugoglobigerina eugubina*
(Luterbacher & Premoli Silva)
GG-75, 86-95 cm
3 *Parvularugoglobigerina eugubina*
(Luterbacher & Premoli Silva)
GG-75, 95-100 cm
4 *Parvularugoglobigerina eugubina*
(Luterbacher & Premoli Silva)
GG-75, 100-110 cm
5 *Eoglobigerina edita* (Subbotina)
GG-75, 100-110 cm
6 *Praemurica pseudoinconstans* (Blow)
GG-75, 882-897 cm
7 *Praemurica pseudoinconstans* (Blow)
GG-75, 882-897 cm
8 *Praemurica pseudoinconstans* (Blow)
GG-75, 882-897 cm
9 *Praemurica pseudoinconstans* (Blow)
GG-75, 882-897 cm
10 *Eoglobigerina edita* (Subbotina)
GG-75, 86-95 cm
11 *Parasubbotina pseudobulloides* (Plummer)
GG-75, 95-100 cm
12 *Parasubbotina pseudobulloides* (Plummer)
GG-75, 100-110 cm
13 *Contusotruncana contusa* (Cushman)
GG-75, Maastrichtian boundary layer
14 *Abathomphalus mayaroensis* Bolli
GG-75, Maastrichtian boundary layer

sponds to the top of calcareous nannoplankton Zone NP1. The duration of Biochron NP1 has been estimated at about 700 ky (Berggren et al. 2000; Gradstein et al. 2004). During this time 805 cm of turbidites, slumps, and hemipelagites were deposited at the Knappengraben section (Lahodynsky 1988b). This suggests a sedimentation rate of 11 mmky^{-1} in the earliest Paleocene.

Lithology of the Gamsbach section

The Gamsbach section (Figs A3.6 and A3.7) consists mainly of fine-grained pelitic rocks. Below the K/Pg light to medium gray marlstones and marly limestones occur (mean carbonate content of 11 samples is 54.9 wt.%; mean content of total organic carbon is 0.18 wt.%), which are interbedded with thin (< 15 cm) sandstone turbidites. Dark gray mottles due to bioturbation are present especially in more indurated marly limestone beds. *Chondrites*- and *Zoophycos*-type burrows were identified. The top of the Maastrichtian consists of 50 cm thick well indurated, bioturbated marly limestone with an irregular, wavy upper surface. Above this surface, 0.2 to 0.4 cm of yellowish clay marks the base of the Paleocene. The yellowish clay is overlain by gray clay with a maximum carbonate content of about 13 wt.% in the upper part of the layer. The overlying 200 cm thick middle to dark gray marl to marlstone contains ca. 20 – 50 wt.% carbonate (mean content of total organic carbon 0.23 wt.%). Twelve thin (0.5 to 5 cm) sandy to silty turbidite layers are intercalated in the first 9 cm of this marlstone. The color of the marls and marlstones changes up-section from light to medium gray, and they are interbedded with brown to reddish layers. Turbiditic beds become thicker there (up to 14 cm). A variegated marl/marlstone bed (40 cm thick) occurs at 323 cm. It contains clasts of red and brown marly limestone up to 15 cm in diameter and some slump folds. Above this mass-flow bed, the grayish-red marl-marlstone succession extends to the top of the section, 400 cm above the K/Pg boundary.

The marly Cretaceous limestones are regarded largely as hemipelagites deposited above the local calcite compensation depth. Turbidity currents disturbed the fine-grained pelagic sedimentation from time to time, delivering sandy and pelitic material into the basin. The less indurated marl beds were deposited by fine-grained tails of sandy-silty turbidity currents or by mud-rich turbidites. This sedimentation pattern continues after the K/Pg boundary with the deposition of marls and thin sandstone turbidites. No clear-cut distinction can be made between turbidite pelites and hemipelagites due to the overall decrease in carbonate content.

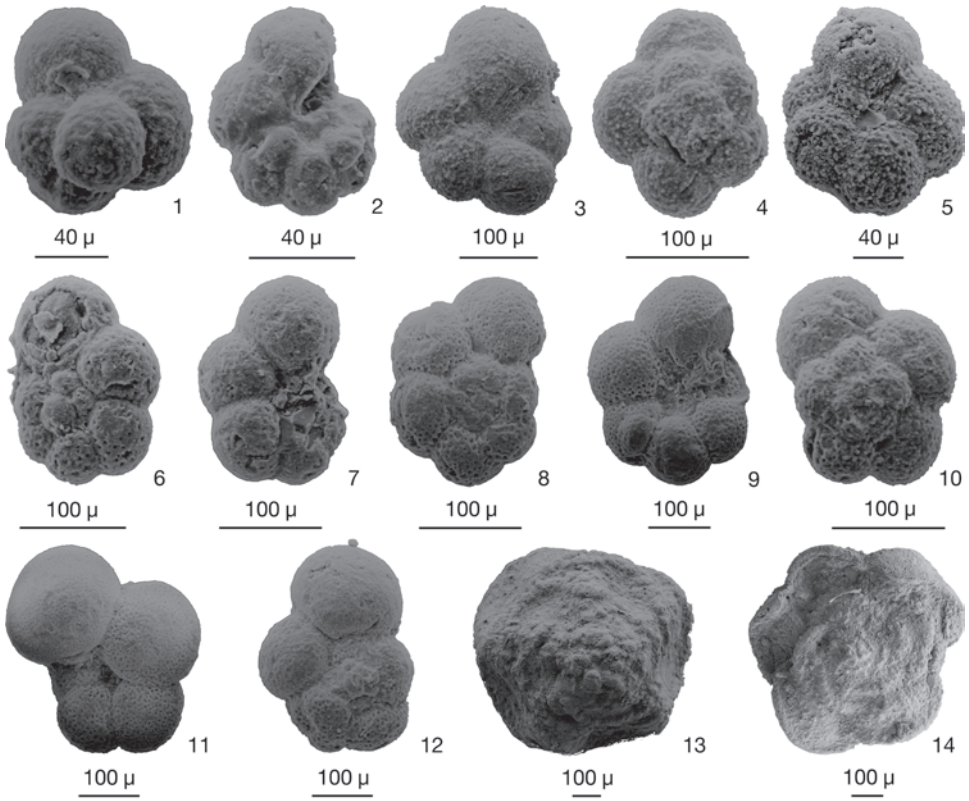

Gams, Knappengraben K/T

Figure A3.6 ►
Photograph of the Gamsbach section. Note that due to higher carbonate contents the Maastrichtian deposits are more resistant to erosion than the Danian ones.

Figure A3.7 ▼
Stratigraphic log of the Gamsbach section, with carbonate content and variation in the stable isotope abundances.

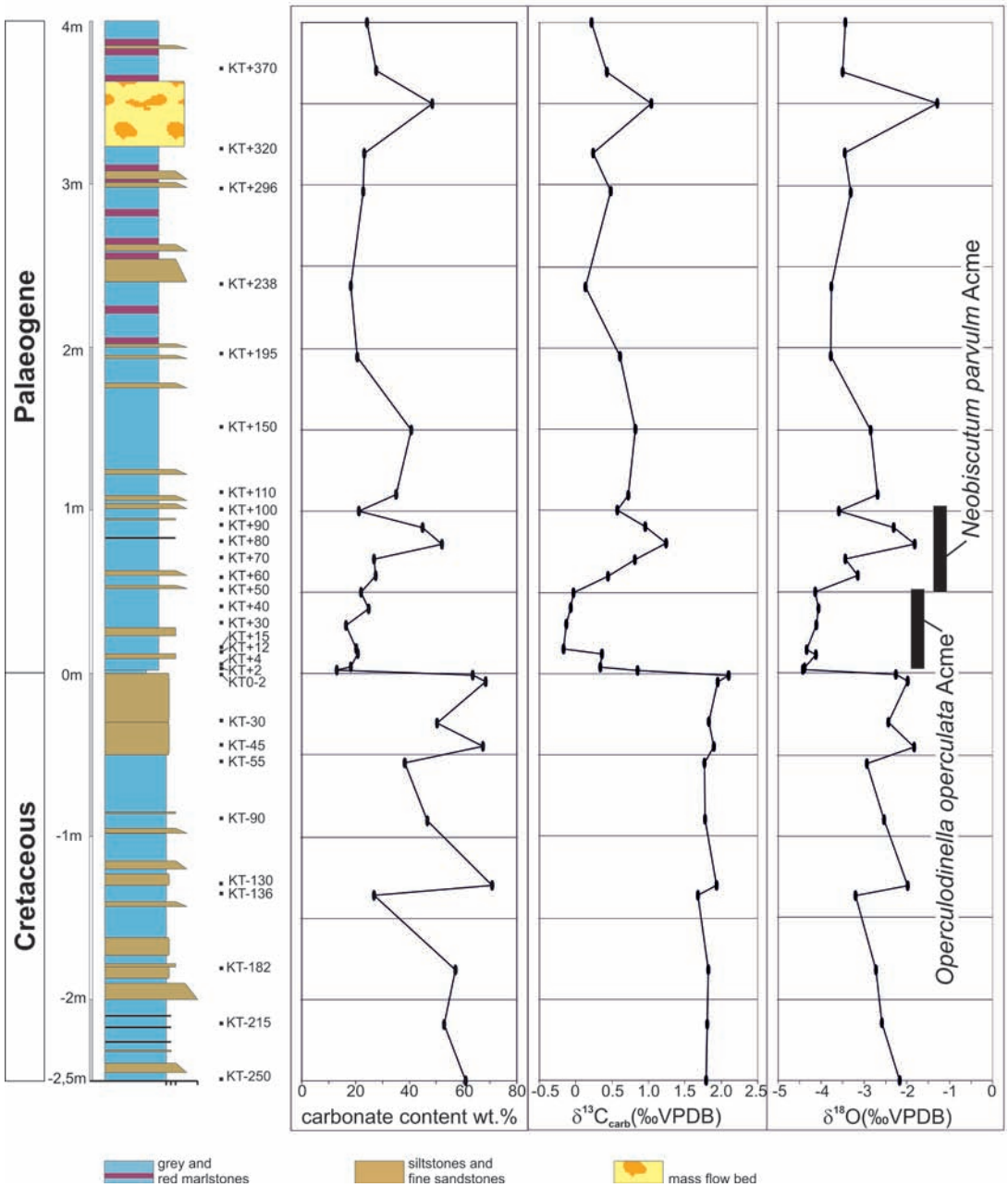

CRETACEOUS CC26									PALEOGENE NP1																	AGE
-250cm	-215cm	-182cm	-136cm	-130cm	-90cm	-55cm	-45cm	-30cm	-0.3cm	+2cm	+4cm	+12cm	+15cm	+30cm	+40cm	+50cm	+60cm	+70cm	+80cm	+90cm	+100cm	+110cm	+150cm	+195cm	+238cm	+296cm	+320cm	+350cm	+370cm	+400cm	SAMPLE KT
5	5	4	6	4	12	14	3	6	4	2	5	5	7	6	8	6	5	7	>100	>100	>100	>100	10	10	15	8	7	3	15	8	ABUNDANCE spp./f.v.
·	·	·	·	·	·	·	·	·	·	·	·	·	·	·	·	·	·	·	·	·	·	·	·	·	·	·	·	·	·	·	*Ahmuellerella regularis*
●	·	·	●	·	■	■	·	●	●	·	·	●	●	·	·	·	·	●	●	●	·	·	·	·	·	·	·	·	●	·	*Arkhangelskiella cymbiformis*
														·			·			·	·		·		·			·			*Biantholithus sparsus*
						·					·	·	·	·	·	·	·	·	·	·	·	·	·	·	·	·	·	·	·	·	*Biscutum constans*
												·					·	·	·	·	·	·									·	*Braarudosphaera bigelowii*
										·		·	·	·			·	·		·	·	·			·		·		·	·	*Broinsonia parca parca*
													·	·	·	·		·	·	·			·			·	·	·	·		*Calculites obscurus*
												·		·											·	·			·	·	*Ceratolithoides aculeus*
	·	·	·		·	·			·				·			·		·								·			·	·	*Ceratolithoides kamptneri*
·	·		·		·	·	·		·	·	·	·		·	·	·	·	·	·		·			·	·	·				·	*Chiastozygus amphipons*
																				·											*Chiastozygus ultimus*
·				·	·	·	·	·	·	·		·	·		·					·	·				·	·			·		*Cribrocorona gallica*
●	·	·	●		●	●	·	●	●	·	·	●	●	·	·	·	·	·	·	·	·	●	·		·	·	·	·	·	●	*Cribrosphaerella ehrenbergii*
			·		·				·		·	·	·	·	·	·	·			·	·	·		·	·	·	·	·	·	·	*Cruciplacolithus primus*
										·	·	·	·	·	·	·	·	·		·	·	·		·	·	·	·	·	·	·	*Cyclagelosphaera alta*
	·					·				·	·	·	●	●	●	●	●	●	●	●	●	●	·	·	·	·		·	·		*Cyclagelosphaera reinhardtii*
												·	·	·	·	·	·	·		·	·	·								·	*Eiffellithus eximius*
·	·	·	·	·	·	·	·	·	·	·	·		·	·	·	·	·	·	·	·		·	·	·	·	●	·	·	·		*Eiffellithus turriseiffeli*
													·	·	·		·			·		·					·				*Goniolithus fluckigeri*
												·	·	·	·	·	·	·	·	·	·	·	·	·	·	·	·	·	●	·	*Lanternithus duocavus*
	·		·		·	·						·	·	·	·				·	·						·	·		·	·	*Lithraphidites carniolensis*
●	●	·	·	·	·	·		·	·		·	·	·		·	·			·	·	·		·		·	·	·			·	*Lithraphidites quadratus*
											·		·	·	·	·														·	*Lucianorhabdus cayeuxii*
																													·		*Manivitella pemmatoidea*
																					·				·	·	·		·		*Markalius apertus*
											·			·	·		·												·	·	*Markalius astroporus*
											·	·	·	·	·	·	·	·	·	·	·	·	·	·	·	·	·	·	·	·	*Markalius inversus*
																						·			·	·	·		·		*Microrhabdulus attenuatus*
·	●	·	·	·	·	·	·	·	·					·	·	·	·			·	·				·			·	·	·	*Microrhabdulus decoratus*
·	·	·	·	·	·	·	·	·	·		·					·					·		·						·		*Micula murus*
·	·		·		·	·			·	·			·			·	·			·	·					·	·	·		·		*Micula prinsii*
●	■	·	■	·	■	■	·	●	■	●	●	●	●	●	●	●	·	·	·	·	●	·	·	●	·	●	●	·	·	●	*Micula staurophora*
						·						·		·				■	■	■	■	■	●	●	●	●	●		·	●	*Neobiscutum parvulum*
											·	·				·	·	·	·	·	·					·					·	*Neocrepidolithus cohenii*
									·		·			·		·	·	·	·	·	·					·	·					*Neocrepidolithus neocrassus*
					·			·	·	·	·	·	·	·		·	·	·	·	·		·		·				·	·	·	*Nephrolithus frequens*
	·				·			·				·			·	·		·	·	·	·					·			·	·	*Octolithus multiplus*
·	·	·	·	·	·	·	·	·		●	●	■	■	■	■	■	■	●	●	●	●	●	●	●	●	●	●	●	●	●	*Operculodinella operculata*
	·		·		·	·	·				·	·	·	·	·	·	·	·		·		·	·	·		·	·	·	·	·	*Placozygus fibuliformis*
												·																			*Petrarhabdus copulatus*
·	·	·	·		●	●	·	●	·	·	·	●	●	·	·	·	·	·	·	·	·	·	·	·	·	·	·	·	●	·	*Prediscosphaera cretacea*
		·			·			·	·			·									·										*Prediscosphaera grandis*
						·			·		·	·		·		·	·					·									*Prediscosphaera spinosa*
						·			·																						*Prolatipatella multicarinata*
			·			·							·			·		·					·						·		*Reinhardtites levis*
·		·			·	·		·	·	·	·	·	·	·	·	·	·	·	·	·	·	·	·	·	·	·	·	·	·	●	·	*Retecapsa crenulata*
					·						·	·			·	·		·				·				·	·			·	·	*Rhagodiscus angustus*
	·							·	·	·	·	·		·				·		·		·		·	·	·			·	·	*Staurolithites crux*
																		·	·					·	·				·		*Tranolithus orionatus*
										·									·												*Uniplanarius gothicus*
									·			·				·										·	·		·		*Uniplanarius trifidus*
●	●	●	●	●	■	●	●	●	●	●	●	●	●	●	●	●	●	●	●	●	●	●	●	●	●	●	·	·	●	●	*Watznaueria barnesae*
			·		·	·									·	·				·	·									·		*Watznaueria biporta*
																		·	·	·		·			·	·			·		*Zeugrhabdotus diplogrammus*
				·		·		·		·		·	·	·	·	·	·								·				·		*Zeugrhabdotus embergeri*
																									·					·	*Zeugrhabdotus sigmoides*

Table 2 ▲
Distribution of calcareous nannoplankton species in the Gamsbach section.
▮ very abundant ■ abundant • common · rare

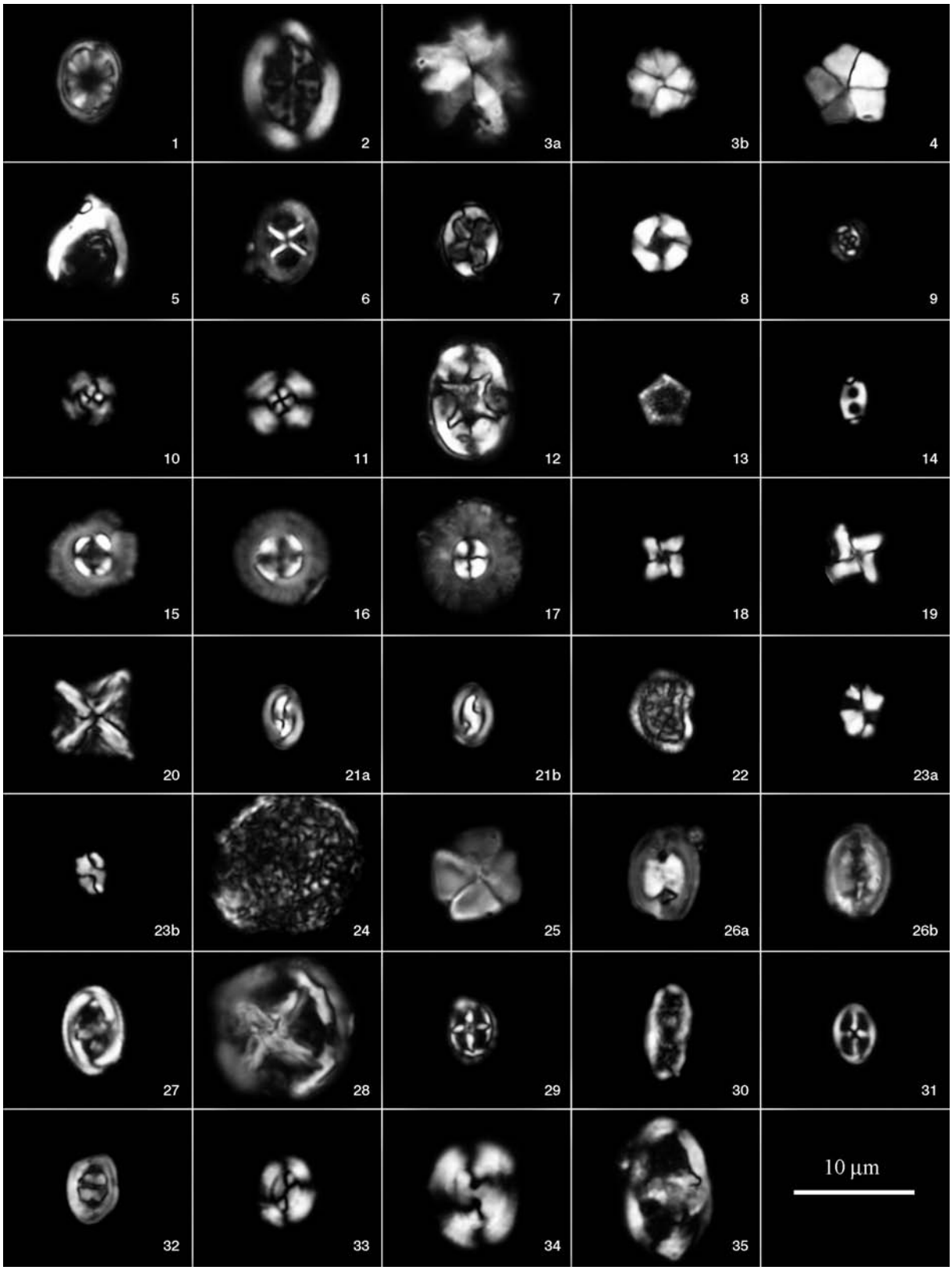

Calcareous nannoplankton

The distribution of calcareous nannoplankton species in 9 samples below and 21 samples above the K/Pg boundary is given in Table 1. Figure A3.7 shows the more important species encountered in the Gamsbach section. The reader is referred to Perch-Nielsen (1985) and Burnett (1998) for taxonomy. The zonal schemes of Martini (1971) and Sissingh (1977) have been used for the Cretaceous and

Figure A3.8 ◄
Calcareous nannoplankton species of the Gamsbach section. All figures were taken with cross-polarized light.

1	*Ahmuellerella regularis* (Gorka 1957) Reinhardt 1966	KT	+370cm
2	*Arkhangelskiella cymbiformis* Vekshina 1959	KT	+4cm
3 a	*Biantholithus* cf *astralis* Bramlette and Martini 1964	KT	+238cm
3 b	*Biantholithus sparsus* Bramlette and Martini 1964	KT	+238cm
4	*Braarudosphaera bigelowii* (Gran and Braarud 1935) Deflandre 1947	KT	+80cm
5	*Ceratolithoides kamptneri* Bramlette and Martini 1964	KT	+370cm
6	*Chiastozygus amphipons* (Bramlette and Martini 1964) Gartner 1968	KT	-0.3cm
7	*Chiastozygus ultimus* Perch-Nielsen 1981	KT	+90cm
8	*Cribrocorona gallica* (Stradner 1963) Perch-Nielsen 1973	KT	+370cm
9	*Cruciplacolithus primus* Perch-Nielsen 1977	KT	+4cm
10	*Cyclagelosphaera alta* Perch-Nielsen 1979	KT	+50cm
11	*Cyclagelosphaera reinhardtii* (Perch-Nielsen 1968) Romein 1977	KT	+60cm
12	*Eiffellithus turriseiffeli* (Deflandre 1954) Reinhardt 1965	KT	+238cm
13	*Goniolithus fluckigeri* Deflandre 1957	KT	+40cm
14	*Lanternithus duocavus* Locker 1967	KT	+370cm
15	*Markalius apertus* Perch-Nielsen 1979	KT	+370cm
16	*Markalius astroporus* (Stradner 1963) Hay and Mohler 1967	KT	+370cm
17	*Markalius inversus* (Deflandre 1954) Bramlette and Martini 1964	KT	+90cm
18	*Micula murus* (Martini 1961) Bukry 1963	KT	-0.3cm
19	*Micula prinsii* Perch-Nielsen 1979	KT	-0.3cm
20	*Micula staurophora* (Gardet 1955) Stradner 1963	KT	+50cm
21 a,b	*Neocrepidolithus cohenii* (Perch-Nielsen 1968) Perch-Nielsen 1984	KT	+90cm
22	*Nephrolithus frequens* Gorka 1957	KT	+12cm
23 a	*Octolithus multiplus* (Perch-Nielsen 1973) Romein 1979	KT	+370cm
23 b	*Octolithus multiplus* (Perch-Nielsen 1973) Romein 1979	KT	+80cm
24	*Operculodinella operculata* (Bramlette and Martini 1964) Hildebrand-Habel, Willems and Versteegh 1999	KT	+40cm
25	*Petrarhabdus copulatus* (Deflandre 1959) Wind and Wise 1983	KT	+12cm
26 a,b	*Podorhabdus? elkefensis* Perch-Nielsen 1981	KT	+12cm
27	*Placozygus fibuliformis* (Reinhardt 1964) Hoffmann 1970	KT	+70cm
28	*Prediscosphaera grandis* Perch-Nielsen 1979	KT	+40cm
29	*Prediscosphaera spinosa* (Bramlette and Martini 1964) Gartner 1968	KT	-0.3cm
30	*Rhagodiscus angustus* (Stradner 1963) Reinhardt 1971	KT	+296cm
31	*Staurolithites crux* (Deflandre and Fert 1952) Caratini 1963	KT	+238cm
32	*Tranolithus orionatus* (Reinhardt 1966) Perch-Nielsen 1968	KT	+80cm
33	*Watznaueria barnesae* (Black 1959) Perch-Nielsen 1968	KT	-0.3cm
34	*Watznaueria biporta* Bukry 1969	KT	-136cm
35	*Zeugrhabdotus embergeri* (Noel 1958) Perch-Nielsen 1984	KT	+50cm

Paleogene deposits, respectively. The Maastrichtian deposits belong to the upper part of the *Nephrolithus frequens* Zone (Zone CC26), which is defined by the co-occurrence of *Nephrolithus frequens* and *Micula prinsii*. The base of the Paleocene consists of the *Markalius inversus* Zone (Zone NP1), which comprises the interval from the lower occurrence (LO) of *Biantolithus sparsus* and/or *Cyclagelosphaera alta* and/or an increased abundance of the calcareous dinoflagellate cyst *Operculodinella operculata* to the LO of *Cruciplacolithus intermedius* (Bernaola and Monechi 2007).

The carbonate values of the Cretaceous samples are about twice as high as those of the Paleogene samples (52 *vs* 25 wt.% on average). The negative aspects of carbonate-rich lithologies on the taphonomy of calcareous nannoplankton are reasonably well known (see Bown et al. 2008, for a review). As a result of post-depositional recrystallization small calcite crystals can be selectively dissolved and larger ones overgrown. These processes may be responsible for the scarcity of small nannoplankton species (e.g., *Biscutum constans*) in the Maastrichtian part of the Gamsbach section, and for the low abundances of calcareous nannoplankton there, ranging from 3 to 14 specimens per field of view. Thirty-three species were identified in total in the Maastrichtian samples. The most abundant species is *Micula staurophora*, followed by *Watznaueria barnesae*. Both species are relatively resistant to dissolution and their large numbers are probably an effect of preservational conditions.

The preservation of the Maastrichtian nannoflora is worse than that of the lower Danian where even very small coccoliths (1 – 3 µm) are well preserved (Fig. A3.9). There, clays isolate nannofossils within an impermeable medium, preventing or inhibiting recrystallization. Due to this better preservation and due to a higher abundance of reworked Campanian species species richness increases from thirty-three species in the Upper Maastrichtian to fifty-five species in the lowermost Paleocene (Table 2). Five new species appear after the terminal Cretaceous event. These new species are *Cyclagelosphaera alta* (LO + 2 cm), *Markalius astroporus* (LO + 4 cm), *Lanternithus duocavus* (LO + 12 cm), *Biantholithus sparsus* (LO + 30 cm), and *Markalius apertus* (LO + 100 cm). *Zeugrhabdotus sigmoides*, another marker spe-

cies for the basal Paleocene, was encountered only in two samples at the Gamsbach section (Table 1). Similar to the North Sea basin, this species seems to be extremely rare in the lower part of Zone NP1 (e.g., Perch-Nielsen 1979; Lottaroli and Catrullo 2000). Other species such as *Cruciplacolithus primus* and *Neobiscutum parvulum*, previously thought to be indicative of the basal Paleocene, have their first appearance date already in the Maastrichtian (Gardin 2002; Mai et al. 2003; Schulte et al. 2006).

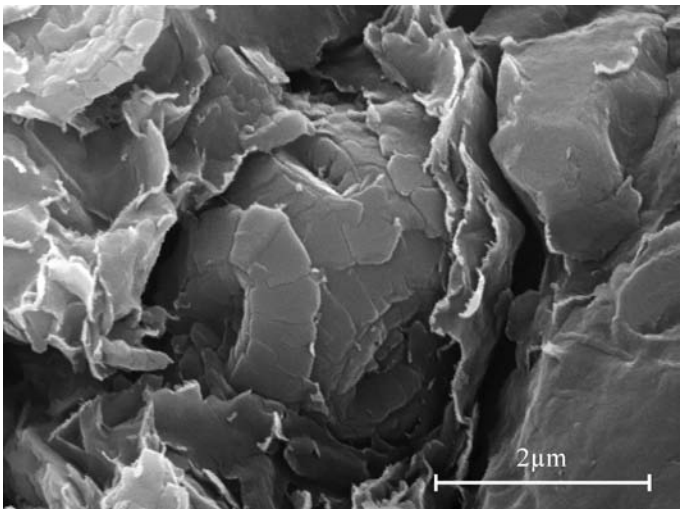

Figure A3.9 ▲
Scanning electron image of a coccosphere of *Neobiscutum parvulum* (Romein 1979) Varol 1989. Note the clay layers coating the fossil. (sample KT+80cm at the Gamsbach section).

The understanding of nannoplankton survivorship is hampered by uncertainties due to massive reworking of Cretaceous species in the Paleocene. In most K/Pg boundary sections reworking of Cretaceous species is clearly restricted to the basal few centimeters of the Danian (Perch-Nielsen 1985). In the Gamsbach section reworked Campanian species were found in all Paleocene samples with the exception of sample KT+350 cm, which originates from a slump. In the other samples the occurrences of *Broinsonia parca parca* and *Eiffellithus eximius* together with *Calculites obscurus*, *Ceratolithoides aculeus*, *Lucianorhabdus cayeuxii*, *Manivitella pemmatoidea*, *Petrarhabdus copulatus*, *Uniplanarius gothicus* and *Uniplanarius trifidus* indicate erosion of Upper Campanian strata at and above the K/Pg boundary. None of these species has been found in the Maastrichtian samples.

Reworking at the Gamsbach section prevents unequivocal differentiation between survivors and victims of the ecological catastrophe at the end of the Mesozoic. Good indicators for survivorship of taxa are atypical abundances of species, reflecting the ecological stress after the rapid environmental changes at the K/Pg boundary (Perch-Nielsen 1985). Albeit scarcely, the calcareous dinoflagellate cyst *Operculodinella operculata* appears regularly in the Maastrichtian samples but exhibits an unprecedented increase in abundance immediately following the K/Pg event. This corresponds to the "*Thoracosphaera*" bloom, which has often been reported in studies of the K/Pg boundary. The cyst-producing genus *Operculodinella* was apparently well adapted to the environmental conditions at and just above the boundary (Hildebrand-Habel et al. 1999).

The maximum abundance of *Operculodinella operculata* in the Gamsbach section is between +12cm and +60cm. Within this interval dominant *Operculodinella* specimens are associated with a significantly increased number of the survivor species *Cyclagelosphaera reinhardtii*.

The *Operculodinella operculata* acme is followed by an acme of *Neobiscutum parvulum* (Fig. A3.9 and Table 2). This species becomes very abundant between +70 cm and +110 cm. More than 100 specimens of this small coccolith species occur per field of view, which is the highest total abundance of calcareous nannoplankton in the entire Gamsbach section. In the other samples the total abundance of *Neobiscutum parvulum* is low varying between 2 and 15 specimens per field of view. *Neobiscutum romeinii* was not recognized at Gams. This may be due to the very small size and low birefringence of this species, which makes it difficult to distinguish it from other *Neobiscutum* specimens.

This distribution pattern of *Operculodinella operculata* and *Neobiscutum parvulum* at the Gamsbach section is similar to that observed at other low-paleolatitude sites (Gardin and Monechi 1998; Gardin 2002; Tantawy 2003; Schulte et al. 2006). A bloom of *Braarudosphaera bigelowii* subsequent to the *Operculodinella* bloom has been described from a number of other K/Pg boundary sites (see Hildebrand-Habel and Streng 2003, for a review). *Braarudosphaera* is a genus, probably favored by high nutrient levels in up-welling or near-shore areas (Kelly et al. 2003; Bown 2005). This palecologic preference may explain the rare occurrence of *Braarudosphaera* specimens in the samples of the bathyal Gamsbach section. The open marine environment can also explain the sporadic occurrence of holococcoliths, because this group prefers neritic settings (Perch-Nielsen 1985). More than 178 dinoflagellate species and subspecies were identified from 89 rock samples concentrated

around the K/Pg boundary. In most samples the dinocysts are moderate to well preserved but associated with reworked material. The dinoflagellate cyst assemblages from most samples are dominated (more than 90%) by gonyaulacoid cysts (e.g., *Spiniferites, Areoligera, Achomosphaera, Hystrichosphaeridium, Adnatosphaeridium, Pterodinium*). Peridinioid cysts occur in low and variable concentrations.

Some well known dinocyst marker species around the K/Pg boundary such as *Carpatella cornuta*, *Spongodinium delitiense, Trithyrodinium evittii, Palynodinium grallator, Manumiella druggii, Cordosphaeridium fibrospinosum, Membranilarnacia? tenella, Senoniasphaera inornata, Damassadinium californicum,* and *Dinogymnium acuminatum* are recorded in the studied samples. These marker species can be correlated with other dinocyst bioevents around the K/Pg boundary in the northern and southern hemisphere. In addition to these, *Trabeculidinium quinquetrum, Lejeunecysta izerzenensis, Batiacasphaera rifensis, Impagidinium maghribensis,* and *Cyclonophelium compactum* represent local markers. A *Spongodinium delitiense* acme is recorded in both studied sections (from 80 cm to 180 cm in Gamsbach section and from 100 cm to 220 cm in Knappengraben section above the K/Pg boundary) and is interpreted as a transient cooling event of oceanic surface waters. The stratigraphic distribution of the dinocyst species indicates that dinocysts have not been seriously affected by the mass extinction event at the K/Pg boundary.

Stable isotopes

Due to the scarcity of marlstone beds in the overall pelitic succession only a moderately high resolution could be achieved for the stable isotope evolution across the K/Pg boundary. No attempt was made to analyze calcareous microfossils separately and we assume that the measured isotope values reflect primarily that of calcareous nannofossils (cf. Perch-Nielsen et al. 1982) plus variable amounts of diagenetically formed calcite cement.

	KT0-2a	KT0-2b	KTK	KTK	KTP	KTP	KTG	KTG
	1	2	3	4	5	6	7	8
Na (wt%)	0.27	0.22	0.19	0.19	0.63	0.62	0.32	0.32
K (wt%)	1.25	0.89	0.86	0.92	2.38	2.50	1.60	1.58
Sc	9.87	7.94	6.37	7.59	16.2	16.6	12.7	12.3
Cr	64.0	48.1	31.3	45.0	121	125	136	131
Fe (wt%)	2.98	2.32	1.50	1.87	4.29	4.42	3.89	3.72
Co	8.67	6.25	18.9	20.8	20.1	20.6	57.2	55.7
Ni	52	46	32	44	74	64	79	84
Zn	94	51	49	60	140	141	129	124
As	2.36	2.63	7.41	7.68	6.90	6.96	42.7	42.3
Se	< 1.4	< 1.2	< 1.1	< 1.3	0.69	< 0.9	< 1.8	< 1.2
Br	0.7	0.6	0.5	0.7	0.5	0.6	0.7	0.8
Rb	75.8	57.9	33.1	55.0	143	137	87	85
Sr	825	712	615	773	239	240	429	390
Zr	141	105	76	117	188	194	161	143
Sb	0.55	0.45	0.54	0.43	1.42	1.14	1.43	1.61
Cs	4.66	3.61	3.08	3.46	8.28	8.16	5.29	5.15
Ba	189	127	97	115	252	249	148	149
La	25.4	22.0	20.0	21.8	23.8	23.1	18.7	18.5
Ce	53.4	46.4	33.5	46.0	46.5	45.6	39.1	38.6
Nd	25.1	21.0	19.5	21.6	21.0	19.2	17.7	18.6
Sm	5.36	4.50	4.10	4.56	4.50	4.28	3.73	3.72
Eu	1.28	1.12	1.03	1.10	0.98	0.96	0.91	0.88
Gd	5.27	4.26	2.97	3.50	4.24	3.75	3.73	3.69
Tb	0.80	0.70	0.48	0.68	0.64	0.60	0.55	0.55
Tm	0.33	0.28	0.25	0.31	0.32	0.31	0.28	0.27
Yb	1.93	1.76	1.57	1.72	1.92	1.84	1.51	1.45
Lu	0.29	0.25	0.23	0.25	0.29	0.29	0.23	0.22
Hf	2.05	1.58	1.28	1.63	4.43	4.71	2.85	2.83
Ta	0.62	0.44	0.34	0.44	1.31	1.27	0.80	0.79
W	1.6	1.4	1.0	1.3	2.8	2.2	2.7	3.0
Os	< 0.2	< 0.2	< 0.2	< 0.2	< 0.3	< 0.2	< 0.3	< 0.3
Ir (ppb)	1.67	0.37	0.34	0.84	4.61	4.25	6.05	5.80
Au (ppb)	0.4	0.4	0.4	0.4	1.5	1.7	2.7	2.6
Th	7.20	5.37	3.66	5.22	13.4	12.9	9.10	9.01
U	0.96	0.71	0.75	0.83	1.75	1.57	1.21	1.20

Table 3 ►
Geochemical data for Gams K/Pg boundary samples. Data by neutron activation analysis. (All data in ppm, except as indicated. Samples: KT0-2a and 2b: shale-textured and compact bulk samples, respectively (thickness about 5cm) just below the K/T-boundary clay; KTK-3 and -4: 2 and 1 cm below the boundary clay, respectively; KTP-5 and 6: 1 and 2 cm above the boundary clay; KTG-7 and -8: duplicate samples of the boundary clay).

The $\delta^{13}C$ values in the uppermost Maastrichtian carbonate beds are rather uniform (ca. +1.8‰) and drop down to values as low as -0.2‰ at the K/Pg boundary. The $\delta^{13}C$ values subsequently increase reaching a maximum of +1.2‰ at +80 cm (Fig. 4). Values then decrease up-section. Higher values are only recorded in components embedded in a slump deposit near the top of the studied section interpreted as reworked Cretaceous sediments.

A similar conspicuous negative shift of 2‰ in $\delta^{13}C$ has been observed in many K/Pg boundary sections, both locally (Gosau basin: Peryt et al. 1997), regionally (Lattengebirge: Perch-Nielsen et al. 1982; Piave River Valley: Fornaciari et al. 2007) and globally (e.g., Zachos et al. 1989; Corfield 1994). This shift implies a rapid and complete collapse of the ocean's bioproductivity which in a normal biologically productive ocean gives rise to a characteristic $\delta^{13}C$ depth gradient, i.e., deep waters being enriched in ^{12}C (e.g., Zachos et al. 1989; Corfield 1994; Kaiho et al. 1999). This earliest Paleocene C isotope minimum is also observed in terrestrial organic matter reflecting a decrease in $\delta^{13}C$ values of atmospheric carbon dioxide (e.g., Maruoka et al. 2007 and references therein).

The $\delta^{13}C$ values largely follow the carbonate content in Gamsgraben, i.e., low $\delta^{13}C$ values coincide with carbonate-poor marls (Fig. 4). The classic model of a 'Strangelove' ocean (Hsü and McKenzie 1985) subsequent to the K/Pg boundary provides an explanation for this correlation, inasmuch as a low-productivity ocean gives rise to a significantly reduced carbonate accumulation rate (cf. Zachos et al. 1989).

The oxygen isotope data show a pattern that is strikingly similar to that of $\delta^{13}C$ (Fig. 4). Maastrichtian $\delta^{18}O$ values (-3.2 to -1.8‰) drop sharply at the K/Pg boundary down to -4.4‰ and remain low in the first 50 cm above the boundary. The values then increase parallel to the $\delta^{13}C$ data (with a maximum at 80cm) and decrease gradually thereafter. A high degree of covariation between both isotope data is commonly regarded as diagnostic of diagenetic alteration, in particular when bulk samples are analyzed. Indeed, scanning electron microscopy has shown that calcareous nannoplankton species from the Maastrichtian of the Gamsbach section commonly exhibit recrystallization and secondary overgrowth. Thus, isotopic reequilibration is implied for that part of the section.

Trace element geochemistry

Eight samples of the boundary section were analyzed by neutron activation analysis. The results are shown in Table 2. Changes in the contents and ratios of other trace elements, such as the rare earth elements (REE), are evident in the layer that marks the K/Pg boundary. The compositions of the samples do not in general change significantly, and most elemental abundance ratios, as well as the chondrite-normalized REE abundance patterns, show values indicative of an upper crustal source. The samples from the boundary clay display relatively lower REE contents than those above and below it, and the boundary sample itself has the lowest Eu value of all of the samples. This was earlier interpreted by Koeberl and Sigurdsson (1992) as being due to REE mobility during palagonitization of the original impact glass spherules deposited after the impact event, and is somewhat similar to the situation described by MacLeod et al. (2007) for the marine K/Pg section at Demerara Rise.

The siderophile elements show a clear maximum at the K/Pg boundary, with maximum values of about 6 ppb Ir, 56 ppm Co, 80 ppm Ni, and 130 ppm Cr. These values are significantly higher than background values below the boundary, and are higher than these in the samples taken just above the boundary clay. The Ir and Co contents indicate about 1 percent by mass of a chondritic component in the sample. The Ni content is somewhat lower than expected, probably due to post-depositional alteration.

Summary

The K/Pg-boundary at the Gamsbach section is characterized by (1) an enrichment of the contents of the siderophile elements Ir, Co, Ni, and Cr compared to the background and continental crustal values, (2) a sudden decrease of carbon and oxygen isotope values, (3) a sudden decrease of carbonate content, and (4) an acme of the calcareous dinoflagellate cyst *Operculodinella operculata*, which is succeeded by an acme of the small coccolith species *Neobiscutum parvulum*. The *Neobiscutum* acme is associated with a positive excursion of $\delta^{18}O$ indicating a transient cooling of ocean surface waters due to short-lived changes in the configuration of ocean circulation after the impact.